THE ASTROPHYSICAL JOURNAL, 403:530–541, 1993 February 1

AN EFFICIENT METHOD TO COMPUTE MICROLENSED LIGHT CURVES FOR POINT SOURCES

HANS J. WITT[1]
Princeton University Observatory, Peyton Hall, Princeton, NJ 08544
Received 1992 May 26: accepted 1992 August 7

ABSTRACT

We present a method to compute microlensed light curves for point sources. This method has the general advantage that all micro images contributing to the light curve are found. While a source moves along a straight line, all micro images are located either on the primary image track or on the secondary image tracks (loops). The primary image track extends from $-\infty$ to $+\infty$ and is made of many sequents which are continuously connected. All the secondary image tracks (loops) begin and end on the lensing point masses. The method can be applied to any microlensing situation with point masses in the deflector plane, even for the overcritical case and surface densities close to the critical. Furthermore, we present general rules to evaluate the light curve for a straight track arbitrarily placed in the caustic network of a sample of many point masses.

Subject headings: gravitational lensing — methods: numerical

1. INTRODUCTION

After the first gravitational lens 0957+561 was found by Walsh, Carswell, & Weymann (1979), Chang & Refsdal (1979) predicted that the brightness changes of a quasar can occur caused by the gravitational lens effect of a *single* star located between observer and source.

This effect was later named *microlensing* since the stars in the deflector plane may split the image of the source into *micro* images which are separated by a few micro-arcseconds. These images are not directly observable but the (dis-)appearance of a pair of micro images yields large brightness changes in the macro image of the lensed quasar which are in fact observable. Each macro image is in this case the unresolved sum of micro images.

To compute the light curve of a given track in the source plane (observer plane), we have to solve the lens equation (see below) for each point of the track. This is easy to do for the case of one star plus shear in the deflector plane, since in this case we can transform this problem to a polynomial of fourth degree. If there is more than one star in the deflector plane, it is not known when a new pair of microimages appears or disappears. The lens equation has to be solved numerically. But one can never be sure that all solutions have been found.

Paczyński (1986) computed light curves for different densities of stars in the deflector plane. He showed that one needs a large amount of computer time to be relatively sure that no (bright) image was missed. Since this method is very time consuming, nobody made improvements on this field. Another computing time–intensive method was developed by Kayser, Refsdal, & Stabell (1986). They use the ray-shooting method to compute light curves for extended sources. This is a very straightforward way to obtain a light curve, and some numerical efforts were done to speed up this method (cf. Schneider & Weiss 1987 and Wambsganss 1990). Nevertheless, this method has the disadvantage that the computing time increases quadratically with the inverse source radius. In fact, Young (1981) might be the first who computed microlensed light curves for extended sources. But unfortunately he gave very few details about his numerical technique.

In 1990 it was shown that for some cases it is useful to use complex quantities instead of two-dimensional vectors for the lens equation of point masses. Using complex quantities a parametric representation of the caustics can be obtained which enables one to compute the whole caustic network of a sample of point masses (Witt 1990). This yields a very efficient method to compute statistics of high magnification events for different samples of point masses (see Witt 1991 and Witt, Kayser, & Refsdal 1992).

In this paper, a new method to compute the light curve of a sample of point masses is presented. This method has the advantage that one is sure that all images which contribute to the light curve have been found without wasting computing time. A similar method was found independently by Lewis et al. (1992). But their numerical technique to compute the light curves is very different from the method described here.

2. THE LENS EQUATION

Microlensing effects are usually described by the normalized lens equation which was first derived by Paczyński (1986) and Kayser et al. (1986). The lens equation describes a mapping from the deflector plane $z = (x, y)$ onto the source plane $\zeta = (\xi, \eta)$. (Bold letters will always describe two-dimensional vectors in this paper.) In this case the normalized lens equation is given by

$$\zeta = \begin{pmatrix} \xi \\ \eta \end{pmatrix} = \begin{pmatrix} 1+\gamma & 0 \\ 0 & 1-\gamma \end{pmatrix} z + \text{sign}\,(\sigma) \sum_{i=1}^{n} m_i \frac{z_i - z}{|z_i - z|^2} \quad (1)$$

where γ is the normalized shear, z_i is the position of the ith star and m_i is the mass of the ith star in units of the solar mass $m_i = M_i/M_\odot$. σ denotes the normalized surface density in stars. It is given as $\sigma = \sigma_*/(1 - \sigma_c)$, where σ_* is the surface density of stars in units of the critical density Σ_{crit} and σ_c is the surface mass density of continuously distributed matter, also in units of Σ_{crit}. For the overcritical case ($\sigma_c > 1$), the normalized surface density σ becomes negative.

The total magnification of a point source is given by the sum of the individual magnifications of each micro image. The mag-

[1] Also Hamburger Sternwarte, Hamburg 80.

nification of an image is given by the inverse of the determinant of the Jacobian of the lens equation (1). Now we obtain

$$\mu_{\rm tot}(\xi, \eta) = \sum_k \mu_k = \sum_k \frac{1}{|\det J|_{z=z_k}} \quad (2)$$

where z_k is the position of the kth image in the deflector plane. The brightness variations (in magnitudes) in the light curve relative to the mean magnification $\langle\mu\rangle = 1/|(1-\sigma)^2 - \gamma^2|$ are given by

$$\Delta m = -2.5 \log (\mu_{\rm tot}/\langle\mu\rangle) . \quad (3)$$

The critical curves in the deflector plane are defined by $\det J = 0$, and the caustics are a mapping of the critical curves onto the source plane. A pointlike source placed on a caustic is infinitely magnified. The caustics divide the source plane into areas with a different number of images. If a caustic is crossed by the source (observer), the number of images changes by 2.

It is well known that the number of images (solutions) of equation (1) can be very different depending on the position of the source (ξ, η) and the normalized surface density σ of the stars. Assuming n point masses in the deflector plane, we obtain a set of real solutions $(x, y)_i$, $i = 1, \ldots, s_r$ for equation (1) which are the positions of the images in the deflector plane. For a given sample of point masses, the number of real solutions s_r depends on the position (ξ, η) of the source in the caustic network. Recently Petters (1992) has shown that $s_r(\xi, \eta) \geq n + 1$ for any given sample of point masses ($\sigma > 0$) and an arbitrary position of the source. In Witt (1990, 1991) it was shown that there also exists a set of complex solutions $(x + \mathrm{i}x, y + \mathrm{i}y)_j$, $j = 1, \ldots, s_c(\xi, \eta)$ for the normalized lens equation. (These solutions can be considered as complex zeros of a real polynomial.) The main point is that the sum $s = s_r + s_c$ of the real and the complex solutions is constant. The sum is given as $s_r(\xi, \eta) + s_c(\xi, \eta) = n^2 + 1$ for no external shear ($\gamma = 0$) and $s_r(\xi, \eta) + s_c(\xi, \eta) = (n+1)^2$ assuming a shear term ($\gamma \neq 0$) (see equation [1]).

3. METHOD

In principle we can search for all real and complex solutions and use only the real solutions to evaluate the light curve. If we do this, we are sure that we have found all real solutions, but we have to waste a lot of computing time searching for complex solutions. We know from experience that usually the number of real solutions is about $n + 1$ to $2n$. In contrast, the number of complex solutions is of order n^2, so this method is not time efficient. We show now another way to find all real solutions using the topological properties of the lens mapping.

3.1. *Some Simple Examples*

To introduce the new method we consider first the simplest case of a point mass with external shear (Chang & Refsdal 1979, 1984). In Figure 1 we show the typical diamond-shaped caustic of a point mass lens with external shear (here: $\gamma = 0.3$) in the source plane. In this paper we assume that the source always moves on a straight line. In the case of static lens configuration, it is sufficient to move only the source to simulate the change in relative position of the source, lens and observer. In Figure 1 five different source tracks are indicated by dashed lines. To apply this method, we have to assume that the tracks are continued over a large range (mathematically speaking from $-\infty$ to $+\infty$). In Figure 2 we show the critical curve (*dashed line*) and the *image tracks* (*solid lines*) which correspond

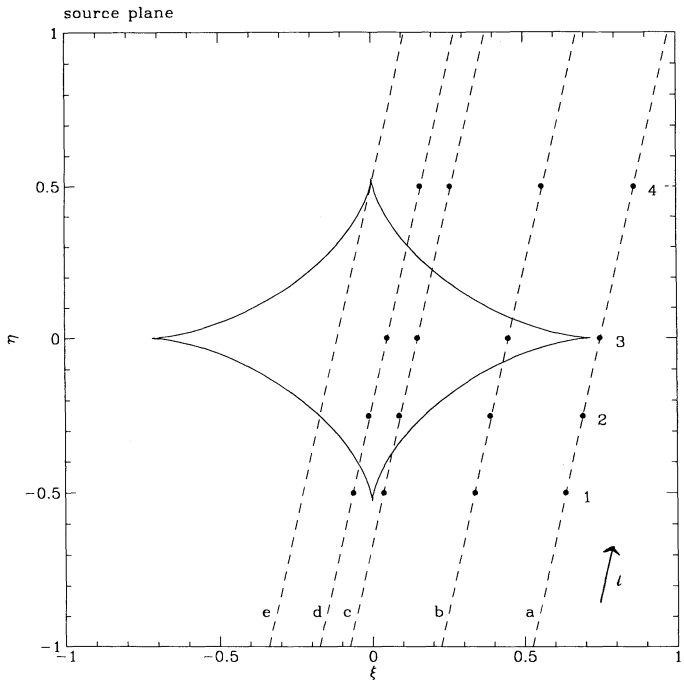

FIG. 1.—Caustic of a single star plus shear ($\gamma = 0.3$) is shown. Five tracks, a–e, are indicated by dashed lines. The arrow indicates the direction of the source.

to the first four source tracks a–d in Figure 1. The image tracks are composed of the solutions of the normalized lens equation for each point on the track in Figure 1. For clarification on each track four positions (1–4) are indicated. They correspond to four different instants of time. In Figure 2 the solutions of these positions are indicated by the same number. These solutions for each instant are the images created by the gravitational lens. The total and the individual brightness (variation) of each image are shown in Figure 3 (see arrows 1–4). The tracks a–d and Figures 1, 2, and 3 are now discussed in detail.

Track a.—It is well known (Chang & Refsdal 1984) that a source placed outside a caustic of a star with shear (i.e. far away) produces two images. One image has negative parity and is close to the star and very faint (see Fig. 3*a*, bottom panel). (The parity of an image is given by the sign of the determinant of the Jacobian of the lens equation; see, e.g., Blandford & Narayan 1986). The other image has positive parity and contributes most of the brightness of this lens system (see Fig. 3*a*, middle panel). (Fig. 3*a* [top panel] shows the total brightness [magnification] of the lens system.) If the source moves from the bottom to the top on track a in the source plane (see the arrow in Fig. 1), then the bright image moves from the bottom to the top as well. It is named the *primary image track* (I); see Figure 2*a*. The other track is named the *secondary image track* (II). In this case, the faint image moves counterclockwise on a loop (compare the numbers 1–4 on track a in Fig. 1 and Fig. 2*a* and look at the arrows). If the source started at infinity, the faint image would start to move at the position of the star. Since for convenience a finite track in the source plane is used there is a small gap in the loop close to the star.

Track b.—The b track is shifted parallel to the a track in the source plane and crosses the caustic. The source moves from the bottom to the top as on track a. We can see in Figure 2*b* that the primary image track crosses the critical curve as well.

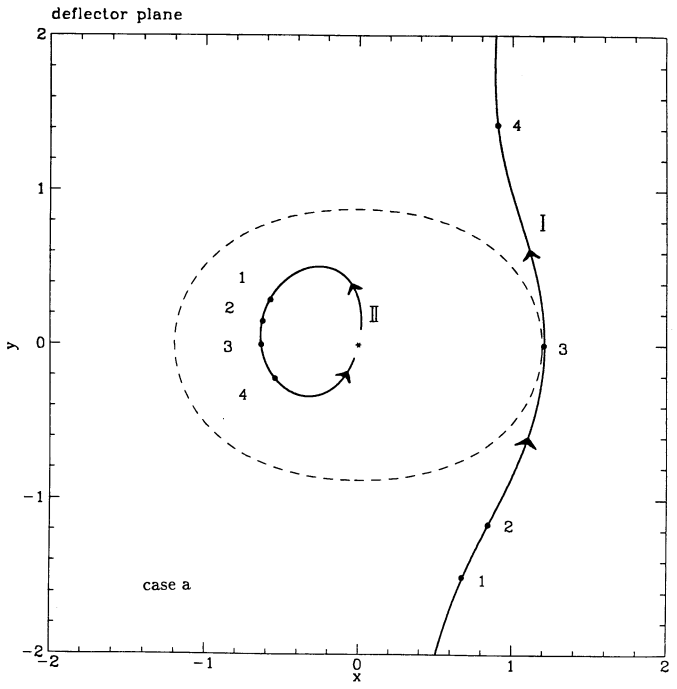

FIG. 2*a*

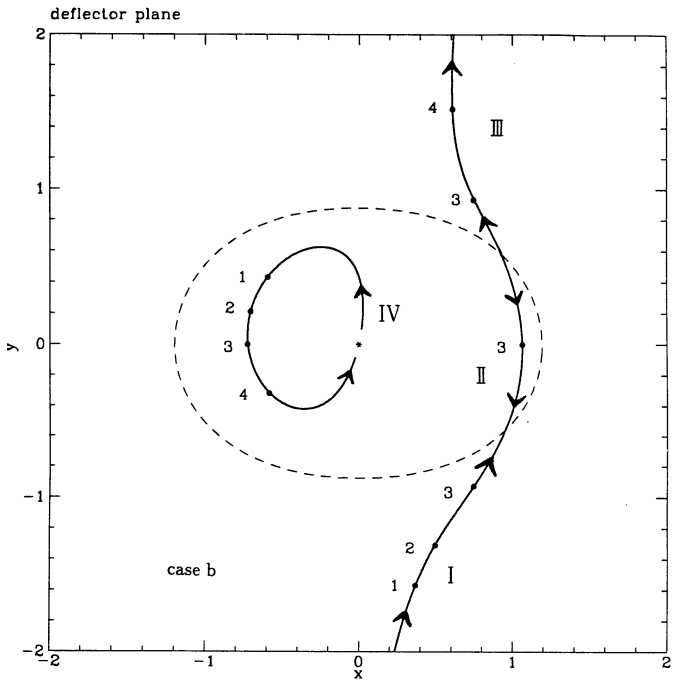

FIG. 2*b*

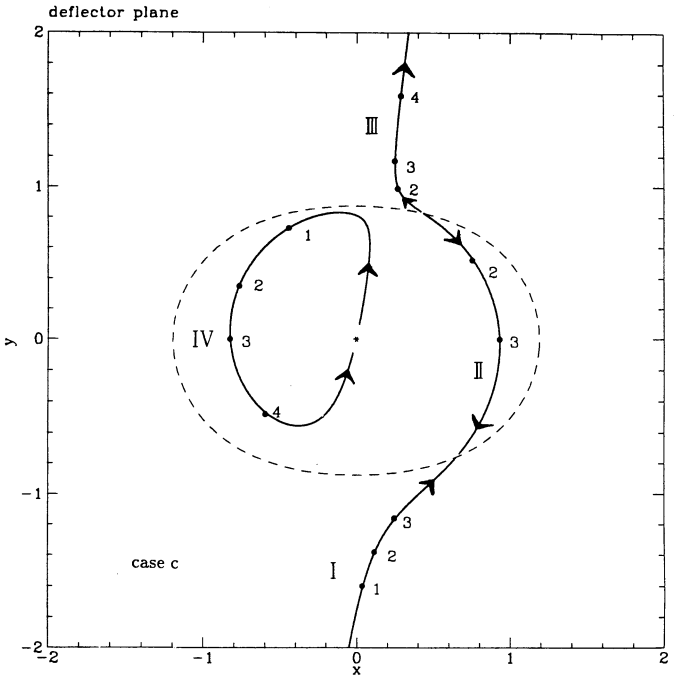

FIG. 2*c*

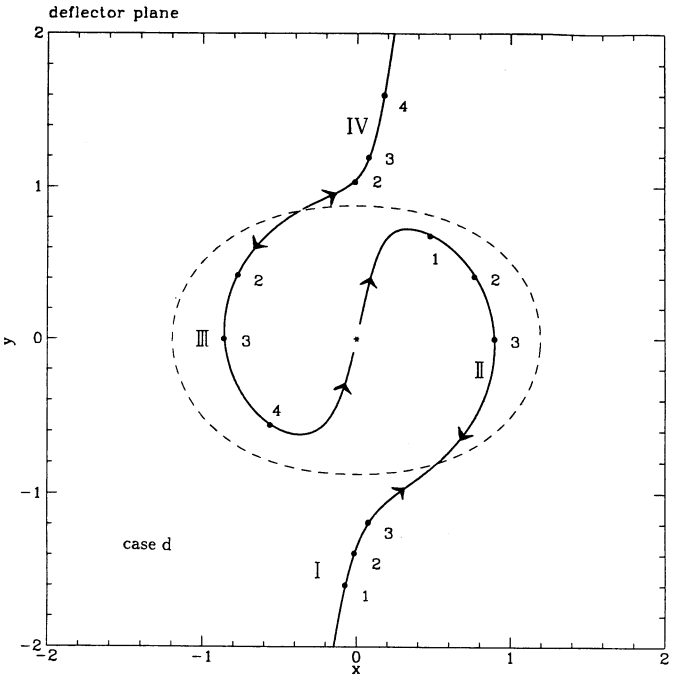

FIG. 2*d*

FIG. 2.—The image tracks due to each source track in Fig. 1 are shown. The critical curve is indicated by a dashed line. The dots labeled by a number denote the solutions (images) for the positions indicated by the same number in Fig. 1. The arrows indicate the direction of motion of the images assuming the source in Fig. 1 moves from the bottom to the top on the source tracks. The asterisk denotes the position of the star.

The arrows on the image tracks indicate the direction of motion of the images. Pairs of images appear and disappear (at different instants of time) at the critical curve, as indicated by the arrows. To compute a complete light curve, the trick is to move in one direction on the image tracks, i.e., not to change the direction of motion on the image track. The (numerical) way to do this is to vary the position of the source step by step along the source track. Simultaneously the variations of the image positions can be found by an iteration function (see § 4). This job is easy to do in case a. But in case b we have to cross a critical curve. Let us assume that we are moving up from the bottom along the image track in Figure 2*b* and that we are crossing a critical curve in the deflector plane for the first time. Then we have to move backwards in the source plane! In Figure 3*b* five different light curves are shown. The light curve at the top is the total sum of the four light curves below. Each

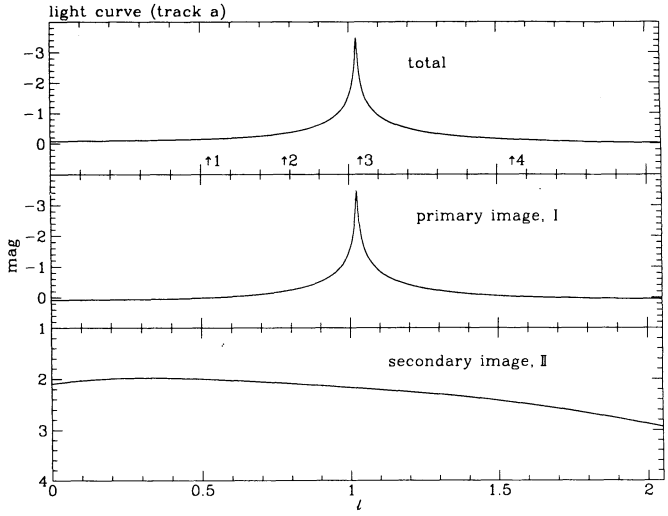

FIG. 3a

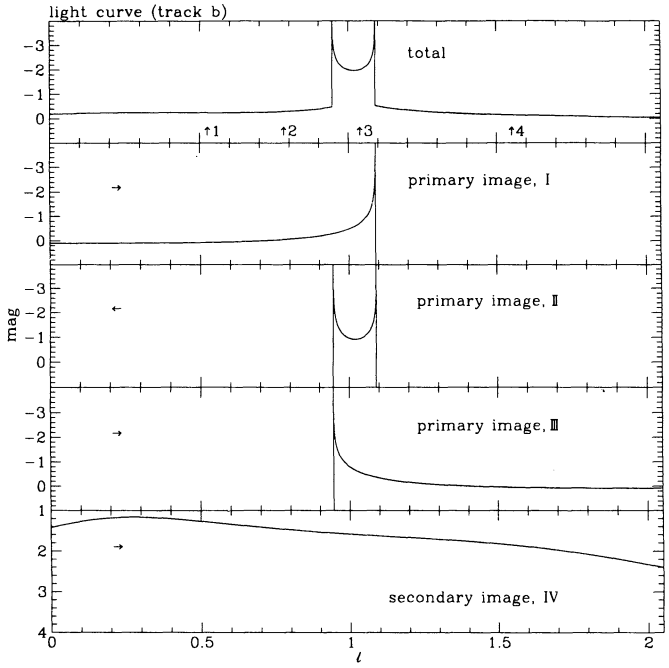

FIG. 3b

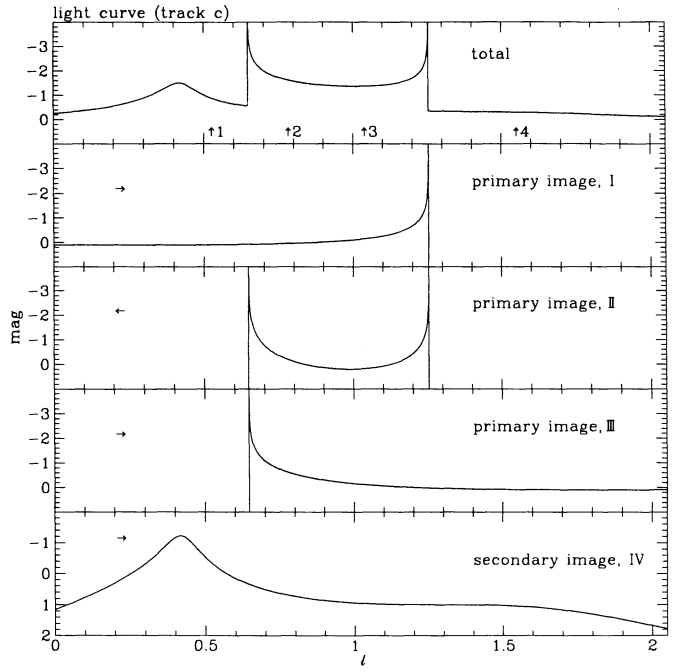

FIG. 3c

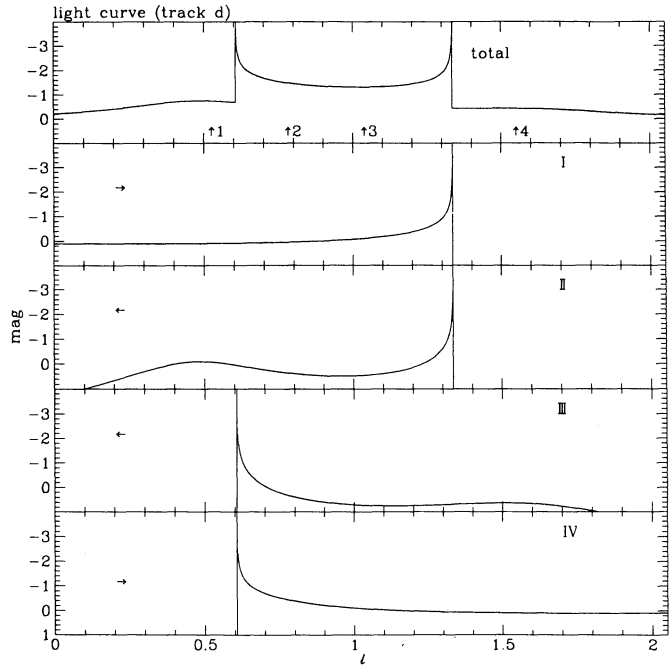

FIG. 3d

FIG. 3.—At each figure the light curve at the top presents the total brightness variation of all images (in a magnitude scale). The light curves at the panels below present the brightness variations of the individual image tracks indicated by a roman number in Fig. 2. The arrows at the top labeled by a number correspond to the position of the source labeled by the same number in Fig. 1. The arrows on the left side below show the direction of motion on the source track during the computation.

of the four light curves below belongs to a part (I–IV) of the image tracks. In Figure 3*b* the direction of motion on the source track is indicated on the left-hand side. The light curve in the middle panel, for example, belongs to part II of the image track inside the critical curve in Figure 2*b* and so on. If we cross the critical curve once more, we have to turn around the direction of motion in the source plane again (move forward). That means that we move 3 times back and forth between the interval of the high-magnification events in the light curve in Figure 3*b*. It is obvious to see in which range four images and in which range two images contribute to the total brightness of the light curve at the top panel. We obtain these individual light curves of each image (second, third, and fourth panel) moving straight on the primary image track but 3 times

back and forward in the interval on the source track. The fourth light curve (*bottom panel*) is obtained by moving along the secondary image track (IV).

Track c.—In Figure 2*c* the secondary image track becomes larger and almost touches the critical curve. Simultaneously the primary image track and the secondary track get closer to each other. Considering the arrows in Figure 2*c* we have to move backward on the source track when we move against the direction of the arrows on the image tracks. We have to move forward on the source track when we move in the same direction as the arrows on the image track. Since the images (dis-)appear only at the critical curve, we have to turn around the direction of motion on the source track whenever we cross a critical curve on the image track (see the light curves in Fig. 3*c*).

Track d.—In Figure 2*d* the two image tracks are merged together into one. A merging (or separation) of two tracks is possible only when the track in the source plane is tangential to a point of the caustic. There is a source track intermediate between c and d which is tangential to the caustic at a point close to the cusp. In that case the secondary and primary image tracks merge. In Figures 4 and 5*b* and 5*c* this case is easier to see. The proof for that is given in § 3.3. If the track d was shifted across the track e to the left, then the image track would separate again into a primary and secondary image track. Then we would get figures similar to Figures 2*a*–2*c*. To compute the light curve we have to move in one direction on the image track (see Fig. 3*d*). If we cross the critical curve the first time, we have to move backward on the source track. In this case we move backward until we reach again the point where we started in the source plane (compare the numbers on the track in Fig. 2*d* and see the second and third panels in Fig. 3*d*). Simultaneously we get close to the star in the deflector plane. To move in one direction on the image track, we have to cross over the star. Simultaneously, we have to start now from the top of the source track and move backward on the source track (compare the numbers on the image track and see the fourth panel in Fig. 3*d*). If we cross once more the critical curve, we have to turn around the direction of motion on the source track (that means we move forward). Finally, we reach again the point at the top in the source plane where we started after we crossed the star (see bottom panel in Figure 3*d*).

In Figure 4 the same caustic is shown as in Figure 1. Three source tracks are indicated, labeled a, b, and c. The track b crosses the caustic 4 times, and tracks a and c crosses the caustic 2 times. In Figures 5*a*–5*c*, the corresponding image tracks are shown. Figure 5*a* shows that in this case the secondary and not the primary image track crosses the critical curve. In Figures 5*b* and 5*c* it is obvious to see that the primary and secondary image tracks merge when the track in the source plane is tangential to the caustic. The light curves for the three tracks are shown in Figures 6*a*–6*c*. The arrows indicate again the direction of motion of the images assuming that the sources moves from the left to the right side of the tracks in Figure 4. The image tracks are computed in the same way as described above.

In Figure 7 we see the caustics of a two-point mass lens without shear. Two tracks are indicated at the top, labeled a and b. In Figures 8*a* and 8*b*, the corresponding image tracks for each case are shown. In this case we obtain three critical curves (*dashed lines*). If the source is positioned outside the caustics, we obtain three images, one of positive parity and two of negative parity close to each star (see, e.g., Schneider & Weiss 1986). Thus we obtain in Figure 8*a* one primary image track, but two secondary image tracks. In Figure 8*b* it is shown that the two secondary image tracks are merged. (Shifting the source track a to the track b in Fig. 7, it becomes once tangential to one point of the caustic. At this moment, the secondary image tracks merge together; see the proof in § 3.3.) For clarification, four positions (instants of time) are indicated in each case on the source tracks in Figure 7. The image positions corresponding to these source positions are indicated by the same number in Figures 8*a* and 8*b*. In Figures 9*a* and 9*b* we see the light curves which correspond to the source tracks in Figure 7. The arrows in the light curves labeled by the four numbers correspond to the positions on the track in Figure 7 labeled by the same numbers.

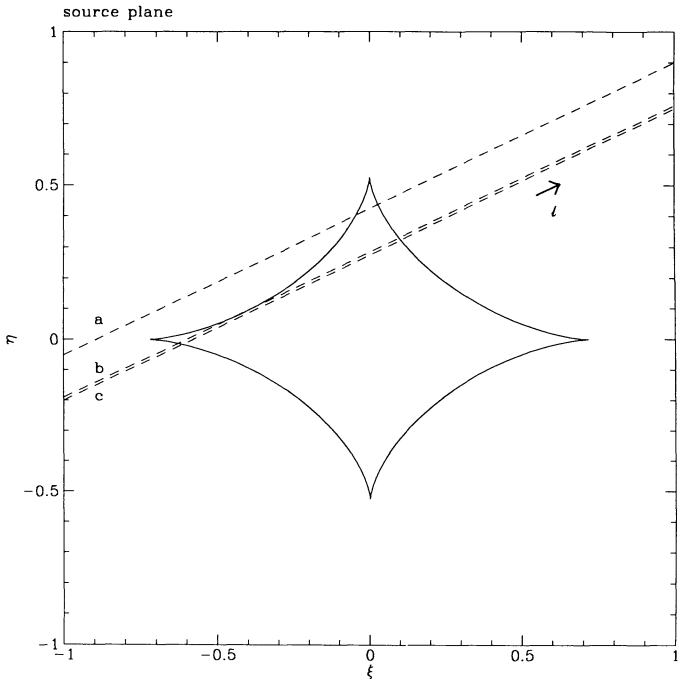

FIG. 4.—Caustic of a single star plus shear ($\gamma = 0.3$) is shown. Three tracks a–c are indicated by dashed lines.

We will see now in the next examples that the features just described in these simple cases completely describe what kind of things can happen in more complicated situations and that these empirical rules are sufficient to compute a light curve due to lensing by a collection of point masses.

3.2. *The General Case*

After discussing the one- and two-point mass gravitational lens in detail, we extend our results to the general case of a gravitational lens with n point masses.

We assume an (infinitely long) track in the source plane which divides the plane into two parts. The track shall be placed in such a way that all caustics are on one side. Then we can shift the track to infinity without crossing a caustic. This means that for each point on the track in the source plane we obtain $n + 1$ solutions in the deflector plane. This is the minimum number of solutions (see Petters 1992). Since we do not cross any caustic, the number of solutions has to be the same for each point on the track in the source plane. Furthermore, we can conclude that in this case we obtain one primary image track and n secondary image tracks, each containing one

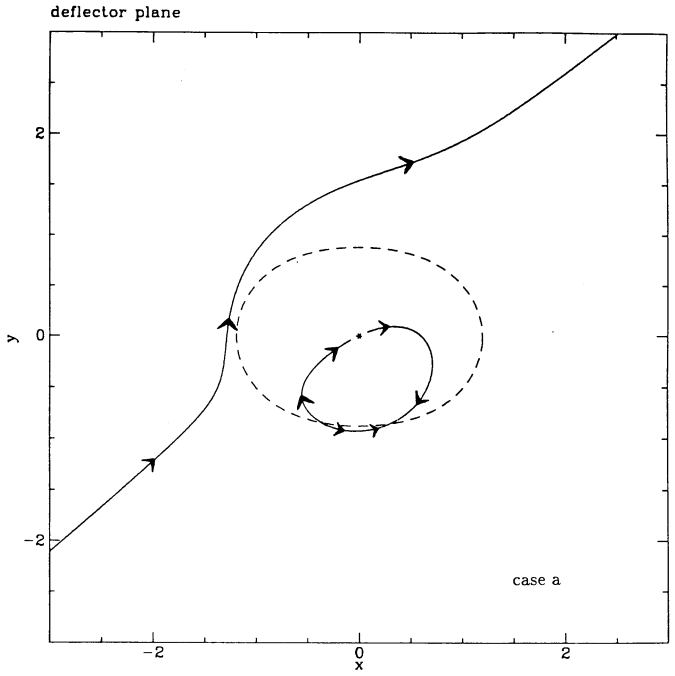

FIG. 5*a*

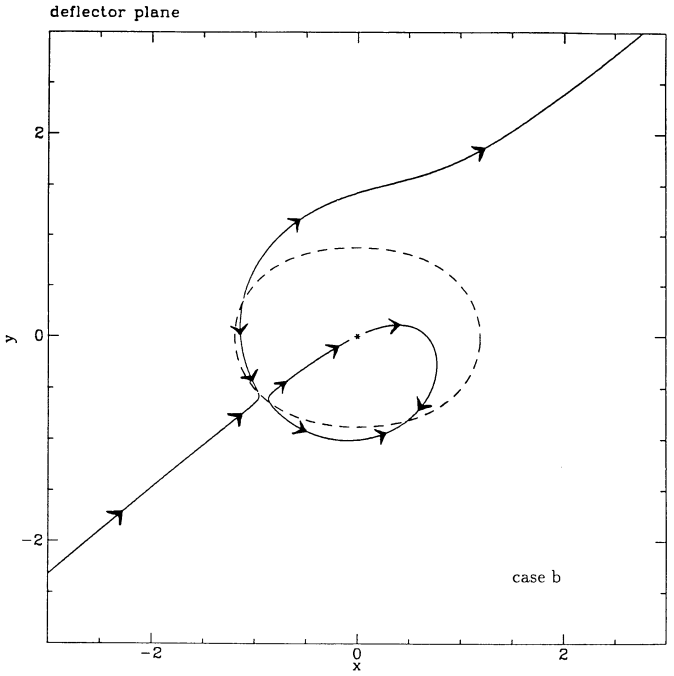

FIG. 5*b*

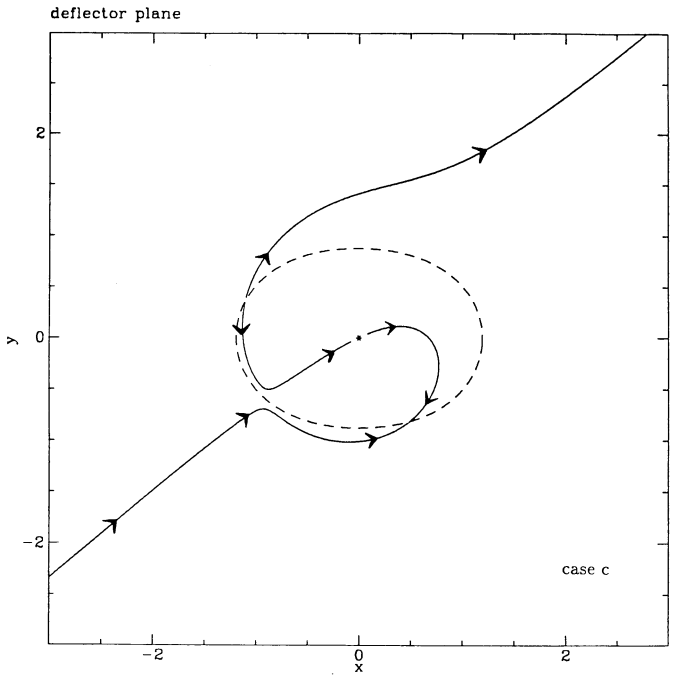

FIG. 5*c*

FIG. 5.—The image tracks due to each source track in Fig. 4 are shown. The critical curve is indicated by a dashed line. The arrows indicate the direction of motion of the images assuming the source in Fig. 4 moves from the left to the right side on the source tracks. The asterisk denotes the position of the star.

star. All secondary image tracks must be separated. In a gedanken experiment, we can always shift the track so far away that the radius of each loop is smaller than the distance to the neighboring star (considering also eq. [12] below) and as long as the track does not get tangential to a caustic no two image tracks can merge (see the proof in the next section).

In the general case of an arbitrary straight track in the source plane we obtain one primary image track and n or fewer secondary image tracks. Each secondary image track must be "connected" with one or more stars, i.e., each secondary image track approaches one or more stars asymptotically while the source is moved to infinity.

To evaluate the light curve we need general rules. For convenience we use a finite track in the source plane. The track has a starting point $\zeta_{\rm start}$ and an end point $\zeta_{\rm end}$. These two points should be far away from any caustic. For computations of

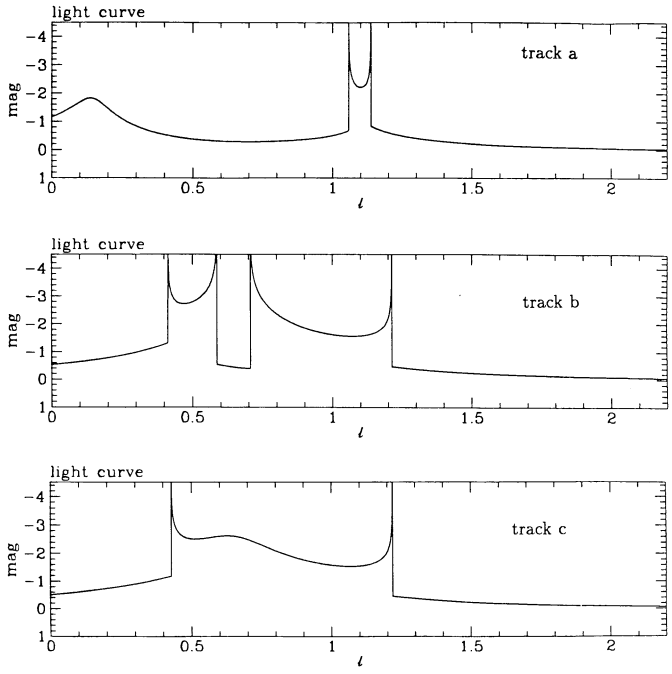

FIG. 6.—Light curves of the three tracks a–c indicated in Fig. 4 are shown

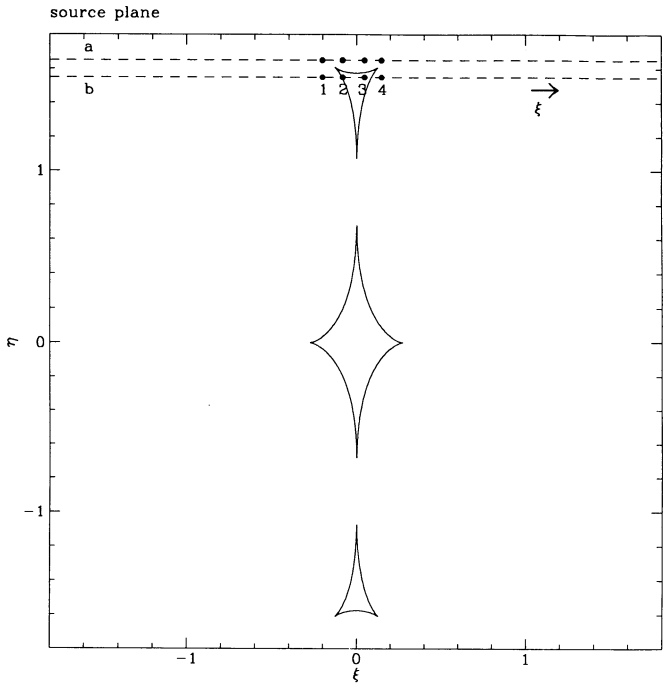

FIG. 7.—Caustics of a two-point mass lens [$z_1 = -z_2 = (0.495, 0)$; $\gamma = 0$] are shown. Two tracks a and b are indicated by a dashed line.

microlensing effects usually the stars (point masses) are randomly distributed in a unit circle. To obtain the normalized density σ inside the circle, the coordinates of the stars are scaled up with a factor $(\Sigma_i m_i/|\sigma|)^{1/2}$. As a rule of thumb for this case it is sufficient to choose $|\zeta_{\text{start}}| \approx |\zeta_{\text{end}}| \approx 2|1 - \sigma|(\Sigma_i m_i/\sigma)^{1/2}$ (for $\gamma = 0$) or $|\zeta_{\text{start}}| \approx |\zeta_{\text{end}}| \gg 1$. Since the starting point is assumed to be outside the caustic network,

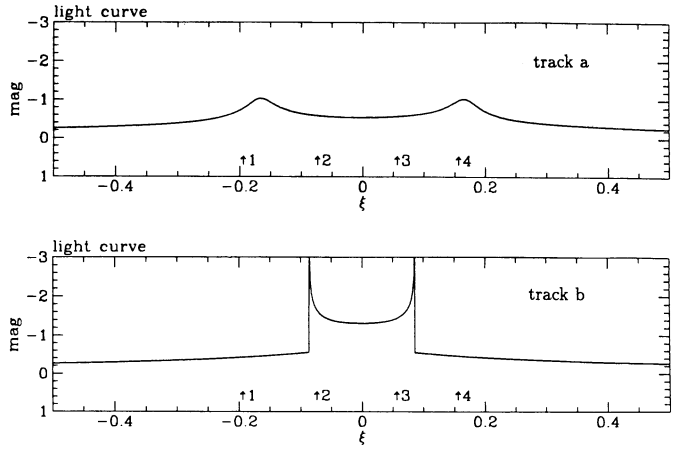

FIG. 9.—The light curves of the two tracks a–b indicated in Fig. 7 are shown. The labeled arrows correspond to the position labeled by the same number in Fig. 7.

we obtain $n + 1$ starting solutions for the image tracks. The n starting position close to the stars (which belongs usually to the secondary image tracks) are well approximated analytically (see eq. [13] below). In general there is one solution (starting position) of positive parity for the case $|\gamma| < 1$ which belongs to the primary image track. For the case $|\gamma| > 1$ there are only starting solutions of negative parity.

Now the (computing) rules for the general case are presented:

1. First, the primary image track has to be computed.
2. If a critical curve is crossed during the computation while following the image track, turn around the direction of motion on the source track.
3. If case 2 happens an odd number of times (that means we

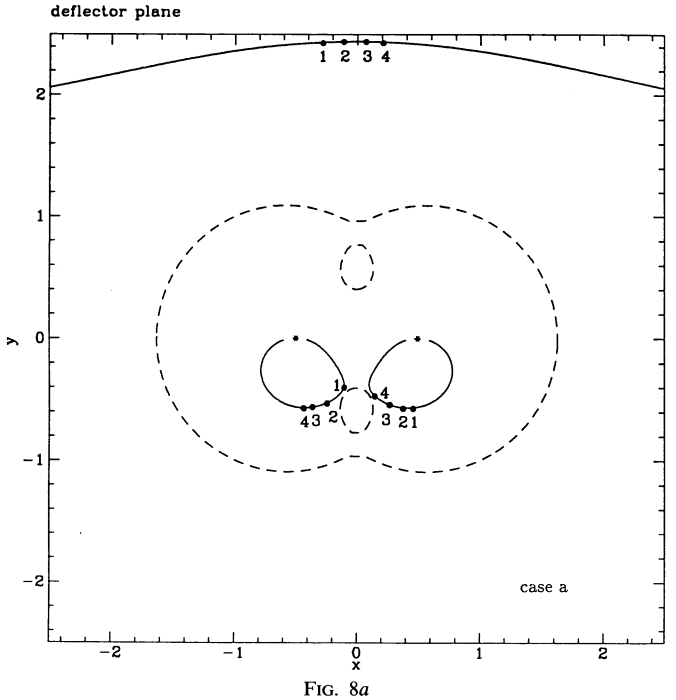

FIG. 8*a*

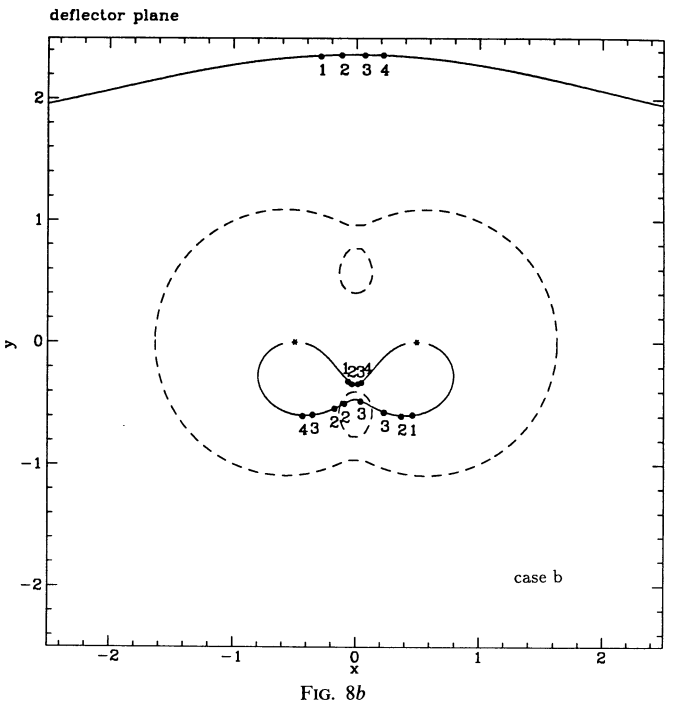

FIG. 8*b*

FIG. 8.—The image tracks corresponding to each track in Fig. 7 are shown. The critical curves are indicated by dashed lines. The numbers denote the solutions (images) for the positions indicated by the same number in Fig. 7. The asterisks denote the position of the stars.

have to move backward on the track in the source plane), the starting point in the source plane is reached again. Simultaneously a starting point of negative parity in the deflection plane very close to a star is reached. Cross the star and move backward from the other side of the track (ζ_{end}) in the source plane.

4. All secondary image tracks can be computed in arbitrary order. Therefore we have to use the n starting points close to the stars and to move on all these image tracks which are connected to each starting point in the deflector plane. If case 3 happened and a starting point of an (original) secondary track is reached, do not use these starting points again during the computation. These starting points (in the deflector plane) have to be excluded for case 4.

5. The computation for every image track is finished only when the end point in the source plane is reached.

These rules are complete and there can not exist loops (secondary image tracks) which are not connected with a star. Therefore, a proof is shown in the Appendix, and another short proof is given in Lewis et al. (1992).

The rules are used to compute the light curve for a sample of 10 point masses. For this case, 10 stars are randomly distributed in a unit circle. In Figures 10*a* and 11*a* (*top panels*), the caustic network for $\sigma = 0.4$ and $\sigma = 0.8$ ($\gamma = 0$) is shown. Furthermore in each case a source track is indicated by a dashed line. [To obtain these densities σ the coordinates of the stars are scaled up with the factor $(10/|\sigma|)^{1/2}$.] In the bottom panel the light curves corresponding to each track are shown. In Figures 10*b* and 11*b* the critical curves (*dashed lines*) and the corresponding image tracks (*solid lines*) are shown. The gaps close to the stars (see the asterisk) appear because we used a finite track in the source plane.

We see that the number of intersections of the image tracks with the critical curve is equal to the number of high-magnification events at the corresponding light curve. For large samples with densities close to 1, we expect a large number of high-magnification events. That means that the image tracks must cross the critical curves the same times. This yields rather complicated image tracks as shown in Figure 11*b*.

This method can also be used for the overcritical case ($\sigma < 0$). In Figure 12*a* (*top panel*) the caustic network for the case $\sigma = -0.4$ for the same sample as in Figure 10*b* is shown. In this case it is absolutely necessary to find all images because there are intervals in the light curve where only faint images contribute to the light curve (see Fig. 12*a*, *bottom panel*). The rules are the same as in the case $\sigma > 0$.

3.3. *Merging of Two Image Tracks*

We consider now the case when the primary track merges with (or separates from) a secondary track or when two secondary tracks merge (or separate). We prove that this happens only if the track (straight line) in the source plane is tangential to a caustic point of the caustic network.

We consider a linear function in the source plane $\eta = a\xi + b$ with arbitrary constants a and b. The image tracks in the deflector plane are given by the implicit function $f(x, y) = a\xi(x, y) + b - \eta(x, y) = 0$ using the normalized lens equation (1). Two

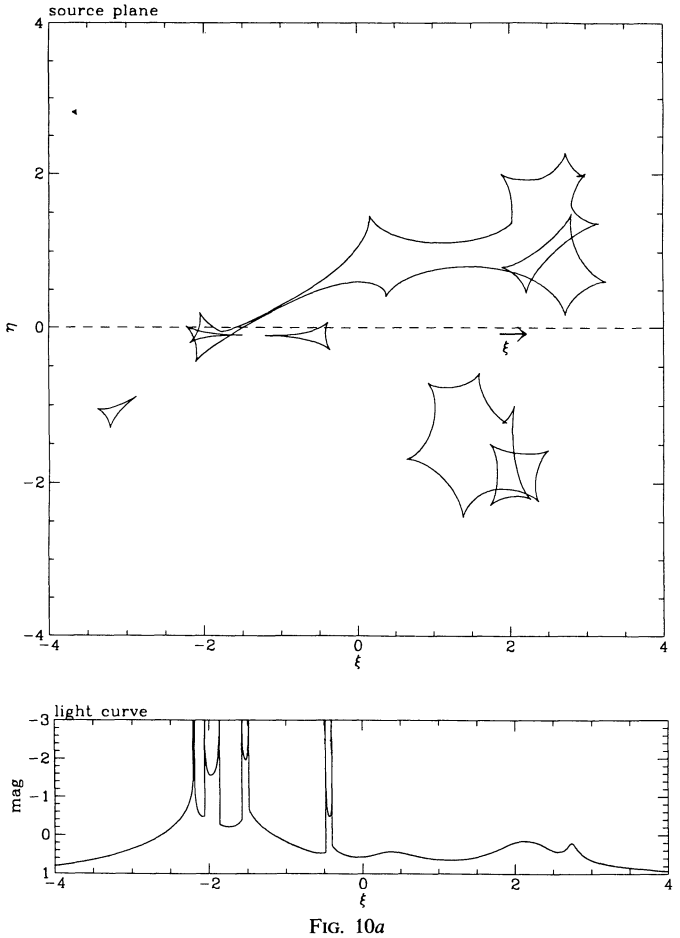

FIG. 10*a*

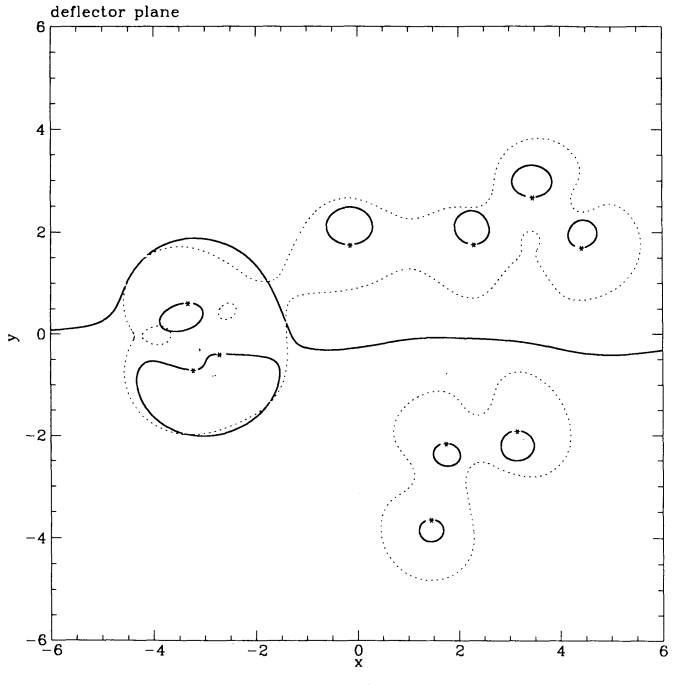

FIG. 10*b*

FIG. 10.—In Fig. 10*a* (*top panel*) a part of the caustic network of a sample of 10 stars ($\sigma = 0.4$, $\gamma = 0$) is shown. A track is indicated by a dashed line. In the bottom panel, the light curve corresponding to the track is shown. In Fig. 10*b* the image tracks due to the track in Fig. 10*a* are shown. The critical curves are indicated by dashed lines.

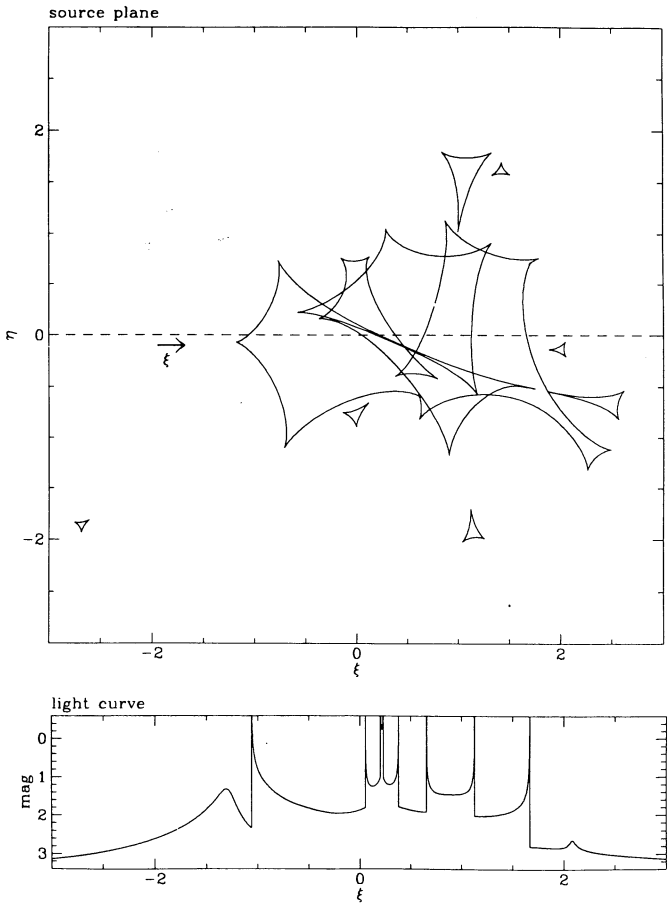

FIG. 11*a*

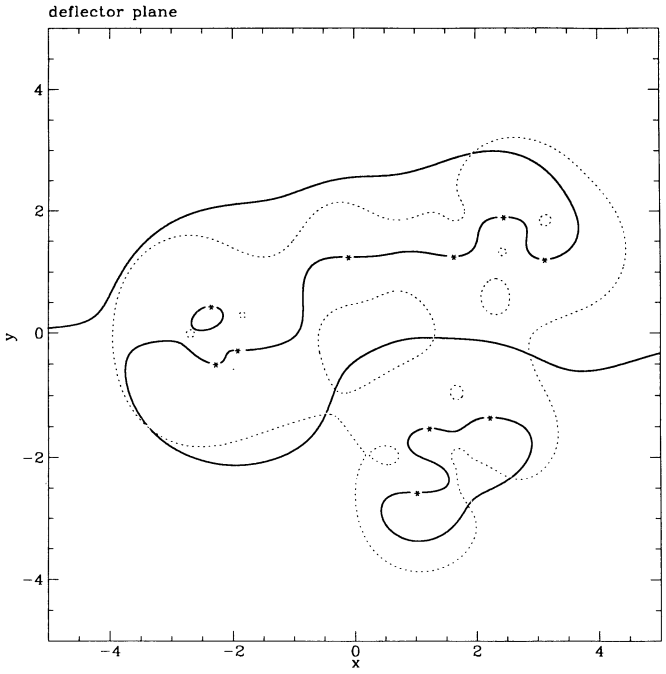

FIG. 11*b*

FIG. 11.—In Fig. 11*a* (*top panel*) a part of the caustic network of a sample of 10 stars ($\sigma = 0.8$, $\gamma = 0$) is shown. A track is indicated by a dashed line. In the bottom panel the light curve corresponding to the track is shown. In Fig. 11*b* the image tracks due to the track in Fig. 11*a* are shown. The critical curves are indicated by dashed lines.

image tracks merge when a tangential vector at the image tracks vanishes. For a merging track we obtain the condition

$$T_{x_{\text{image track}}} = -\frac{\partial f}{\partial y} = -a\frac{\partial \xi}{\partial y} + \frac{\partial \eta}{\partial y} = 0 \tag{4}$$

$$T_{y_{\text{image track}}} = \frac{\partial f}{\partial x} = a\frac{\partial \xi}{\partial x} - \frac{\partial \eta}{\partial x} = 0\,. \tag{5}$$

These two equations can only be true if the two equations are linearly dependent; that means

$$\det A = \frac{\partial \xi}{\partial y}\frac{\partial \eta}{\partial x} - \frac{\partial \eta}{\partial y}\frac{\partial \xi}{\partial x} = 0 \tag{6}$$

But equation (6) is identical to the determinant of the Jacobian of the lens equation and gives the condition for the critical curves. That means that two image tracks can merge only at a critical curve.

We only have to prove now that the linear track in the source plane must be parallel to the corresponding point on the caustic. Therefore we consider a tangential vector $\boldsymbol{T}_\zeta$ at the caustic. It is given by (see Chang 1984 and Kayser & Witt 1989)

$$\boldsymbol{T}_\zeta = \begin{pmatrix} T_\xi \\ T_\eta \end{pmatrix} = J\boldsymbol{T}_z = J\begin{pmatrix} T_x \\ T_y \end{pmatrix} = J\begin{pmatrix} -\dfrac{\partial \det J}{\partial y} \\ \dfrac{\partial \det J}{\partial x} \end{pmatrix}, \tag{7}$$

where $\boldsymbol{T}_z$ is the corresponding tangential vector at the critical curve. If equations (4) and (5) are true then the following vector product must vanish:

$$\begin{pmatrix} T_\xi \\ T_\eta \\ 0 \end{pmatrix} \times \begin{pmatrix} 1 \\ a \\ 0 \end{pmatrix} = \begin{pmatrix} 0 \\ 0 \\ T_\xi a - T_\eta \end{pmatrix}. \tag{8}$$

Inserting equation (7) in the third component of the vector we obtain

$$a\left[\frac{\partial \xi}{\partial x}T_x + \frac{\partial \xi}{\partial y}T_y\right] - \left[\frac{\partial \eta}{\partial x}T_x + \frac{\partial \eta}{\partial y}T_y\right] = \left[a\frac{\partial \xi}{\partial x} - \frac{\partial \eta}{\partial x}\right]T_x + \left[a\frac{\partial \xi}{\partial y} - \frac{\partial \eta}{\partial y}\right]T_y = 0\,. \tag{9}$$

It was not mentioned that we have to assume that the tangential vector at the caustic is well defined. This assumption holds at a fold caustic since $\boldsymbol{T}_\zeta \neq 0$. But at a cusp we obtain $\boldsymbol{T}_\zeta = 0$ which means the direction of the tangential vector is not defined. But we can treat this point as a removable singularity. Therefore we define that a given track is tangential to a cusp when the track and the cusp point in the same direction.

4. NUMERICAL METHOD

For the computation of the image tracks, it is not absolutely necessary but substantially more convenient to use complex

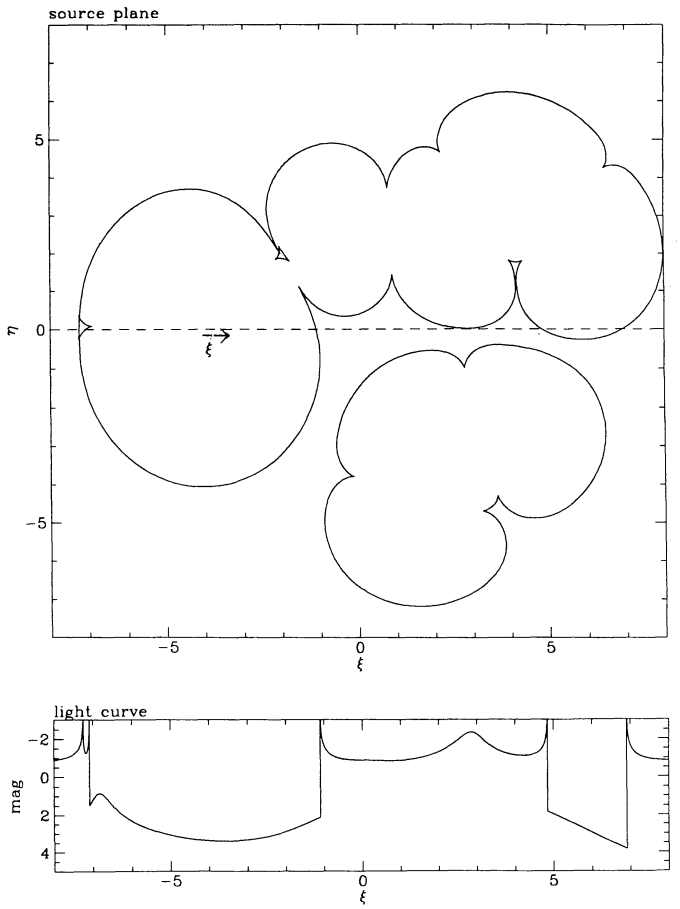

FIG. 12*a*

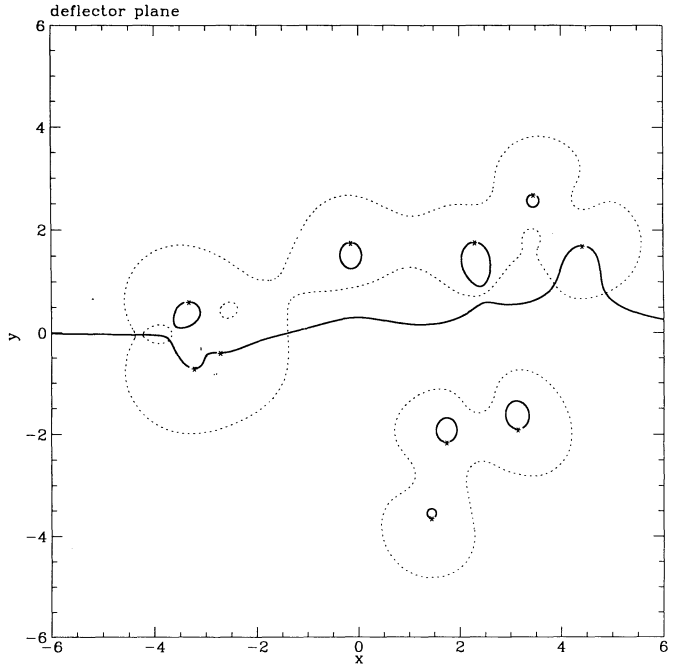

FIG. 12*b*

FIG. 12.—In Fig. 12*a* (*top panel*) a part of the caustic network for the overcritical case of a sample of 10 stars ($\sigma = -0.4$, $\gamma = 0$) is shown. A track is indicated by a dashed line. In the bottom panel, the light curve corresponding to the track is shown. In Fig. 12*b* the image tracks due to the track in Fig. 12*a* are shown. The critical curves are indicated by dashed lines.

quantities. Using the complex quantities $z = x + iy$ and $\zeta = \xi + i\eta$ the normalized lens equation (1) can be written as

$$\zeta = z + \gamma\bar{z} + \text{sign}\,(\sigma) \sum_{i=1}^{n} \frac{m_i}{\bar{z}_i - \bar{z}}, \tag{10}$$

where $\bar{z}$ is the complex conjugate of z.

To compute all image tracks we need the starting points in the deflector plane corresponding to the starting point on the track in the source plane. As discussed above for the case $|\gamma| < 1$ there exists one starting point of positive parity which belongs to the primary image track and n starting points of negative parity very close to each star.

To find the solution for the starting point of positive parity which belongs to the primary image track, a fixed point iteration method is used. (To distinguish between the position of the stars z_i and the number of iterations, the index of the number of iterations is put into brackets.)

$$z_{[k+1]} = f(\bar{z}_{[k]}) = \zeta_{\text{start}} - \gamma\bar{z}_{[k]} - \sum_{i=1}^{n} \frac{m_i}{\bar{z}_i - \bar{z}_{[k]}}. \tag{11}$$

This method converges very fast and a rough estimate of $z_{[0]}$ is adequate. (This method is only convergent if $|\partial f/\partial\bar{z}| < 1$ which is only true for images of positive parity. For the case $|\gamma| > 1$ we have to use eqn. [14] below to find the starting point of the primary image track.)

The n positions of negative parity close to the stars can be estimated in the following way. Assuming $|\zeta_{\text{start}}| \gg 1$ each solution is at position $z = z_l + \epsilon_l$, $l = 1, \ldots, n$, where $|\epsilon_l| \ll 1$ is very small. Now we obtain

$$\zeta_{\text{start}} = z_l + \epsilon_l + \gamma(\bar{z}_l + \bar{\epsilon}_l) + \sum_{\substack{i=1 \\ i\neq l}}^{n} \frac{m_i}{\bar{z}_i - \bar{z}_l - \bar{\epsilon}_l} + \frac{m_l}{\bar{z}_l - \bar{z}} \tag{12}$$

If we drop the ϵ and solve the equation for z we obtain fairly exactly the n starting positions of negative parity:

$$z \approx z_l - m_l \Big/ \left[\bar{\zeta}_{\text{start}} - \bar{z}_l - \gamma z_l - \sum_{\substack{i=1 \\ i\neq l}}^{n} \frac{m_i}{z_i - z_l}\right] \quad l = 1, \ldots, n. \tag{13}$$

After we have found all the starting points we have to evaluate the primary image track first. Now we have to move step by step on the track in the source plane and simultaneously we have to compute the solutions on the primary image track. The steps are defined as $\zeta_j = \zeta_{\text{start}} + j\Delta\zeta$, $j = 1, \ldots, N$ where $\Delta\zeta =$

$(\zeta_{end} - \zeta_{start})/N$. N has to be chosen very large and usually about 1000 steps per unit length in the source plane are taken.

To obtain the solutions on the image tracks a two-dimensional Newton iteration function is used which was transformed into the complex manner. For the complex lens equation (10) we obtain

$$z_{[k+1]} = z_{[k]} - \frac{1}{\det J}\left(\zeta - \frac{\partial\zeta}{\partial\bar{z}}\bar{\zeta}\right), \tag{14}$$

where

$$\det J = 1 - \frac{\partial\zeta}{\partial\bar{z}}\frac{\overline{\partial\zeta}}{\partial\bar{z}} \tag{15}$$

is the determinant of the Jacobian (see Witt 1990). The iteration function in equation (14) can always be used even very close to the critical curve.

The most difficult case is to cross the critical curve (and turn around the direction of motion in the source plane) since there are two positions of convergence very close together. It is known that if the source crosses the caustics a pair of micro-images appears at the critical curve which have the same brightness (magnification), but different signs of the determinant of the Jacobian (see, e.g., Chang 1984 and Blandford & Narayan 1986). (If the source moves away from the caustic, one image becomes usually very faint and the other remains bright.) To find the solution on the other side of the critical curve, we have to move on the isolines of same magnification, but opposite parity. These isolines of constant magnification in the deflector plane are given by the following parametric representation. (This parametric representation is very similar to that of the critical curves where $\det J = 0$; compare Witt 1990).

$$\frac{\partial\zeta}{\partial\bar{z}} = e^{i\varphi}\sqrt{1 - (\pm)|\det J|}\,; \quad \varphi \in [0, 2\pi)\,. \tag{16}$$

Using this equation and varying the parameter φ smoothly, we obtain different values of z, where one of these values is the solution we searched for. To find this solution we only have to check if equation (10) is fulfilled.

5. DISCUSSION

A new method is presented in this paper which enables one to compute microlensed light curves for point sources. This method has the general advantage that one finds every image which contributes to the light curve without wasting computing time. There are several examples discussed. The trick to compute a light curve of a limited track in the source plane is to continue this track to infinity. The solutions in the deflector plane of this (infinitely long) track are continuous image tracks without gaps. A straightforward method to compute all image tracks is presented. These image tracks finally yield the total magnification one obtains at each point on the track in the source plane.

Furthermore a proof is given that two of these image tracks can only merge (or separate) when the track in the source plane is tangential to a point on the caustic network.

We hope that this method will enable us to investigate in more detail the structure of the light curves and the properties of microlensing. This method is not only useful to compute light curves for point sources. It can be used in different ways to obtain light curves for extended sources from the light curves of point sources. We like to mention some further examples where this method could be applied:

1. It can be used to compute the probability $P(\mu > \mu_0)$ to obtain a magnification greater than μ_0 at a random point in the observer plane (see also Paczyński 1986 and Wambsganss 1992). For (very) large μ_0 this result is obtained analytically (see Schneider 1987 and Peacock 1986). But it is still not understood in what kind of ranges of magnification these formulae can be applied. Only for low surface densities were first investigations done (see Rauch et al. 1992).

2. The influence of cusps on the frequency of high-magnification events (see Wambsganss, Witt, & Schneider 1992) and the magnification cross section of a cusp can be computed by this method. These numerical results could be compared with the analytical investigations by Mao (1992) and Schneider & Weiss (1992).

It is a pleasure to thank Tomislav Kundić, Bohdan Paczyński, and Joachim Wambsganss for their careful reading of the manuscript and many helpful suggestions. This project was in part supported by NASA grants NAGW-2448 and NAG5-1901 and in part by a research fellowship of the Deutsche Forschungsgemeinschaft (DFG) under Az. Wi 1122/1-1.

APPENDIX

We show now that all loops (secondary image tracks) must be connected with at least one star. Since Lewis et al. (1992) give a very short proof of that, only a short description of another proof with a very different viewpoint is given.

For the proof we use equation (A3) in Witt (1990). This equation maps all complex and real images on one two-dimensional plane. That means that we obtain additional image tracks from the complex (not observable) images. In this case the number of images is conserved. No images can appear or disappear. As mentioned before the total number of images is always $n^2 + 1$ for $\gamma = 0$ or $(n + 1)^2$ for $\gamma \neq 0$, because equation (A3) of Witt (1990) is equivalent to a complex polynomial of degree $n^2 + 1$ or $(n + 1)^2$, respectively. (n is the number of stars in the lens plane.)

The proof is described for the case of one star plus external shear. In this case we obtain for equation (A3) (Witt 1990) ($\sigma > 0$)

$$(\gamma - \gamma^3)z^4 + (2\gamma^2\bar{\zeta} - \bar{\zeta} - \gamma\zeta)z^3 + (2\gamma^2 + \zeta\bar{\zeta} - \gamma\bar{\zeta}^2)z^2 + (\zeta - 2\gamma\bar{\zeta})z - \gamma = 0\,; \tag{A1}$$

see also Mao (1992, eq. [4]). Figures 13*a* and 13*b* show the image tracks of equation (A1) for the source tracks a and b of Figure 1. Comparing Figure 13*a* with Figure 2*a*, one finds two additional image tracks which belong to the two complex solutions. The number of (real plus complex) images is always four in this case. If we move the source to infinity in Figures 13*a* or 13*b*, two images (solutions of eq. [A1]) move also to infinity and two images get close to the star.

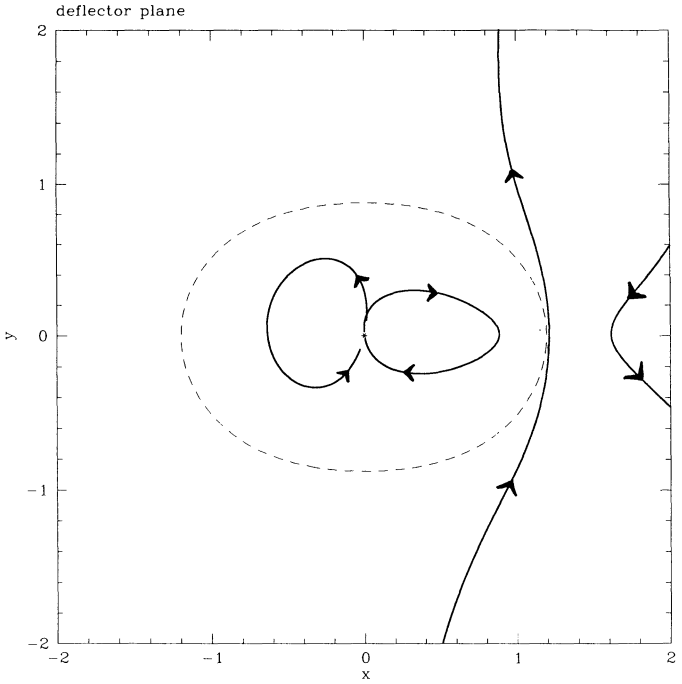

FIG. 13*a*

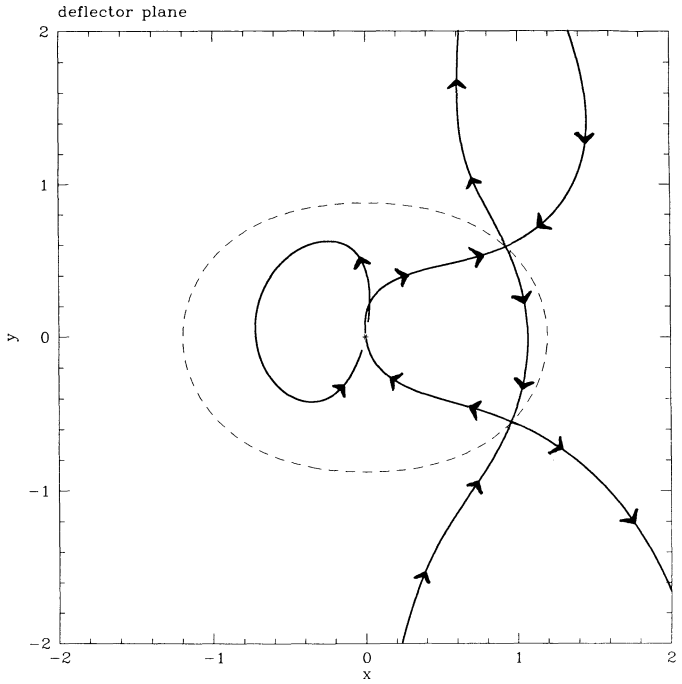

FIG. 13*b*

FIG. 13.—The image tracks due to source track a and b in Fig. 1 are shown. In contrast to Figs. 2*a* and 2*b* all image tracks (complex and real solutions) are shown (see the explanation in the Appendix). The critical curve is indicated by a dashed line. The arrows indicate the direction of motion of the images assuming the source in Fig. 1 moves from the bottom to the top on the source tracks. The asterisk denotes the position of the star.

In general if we move the source to infinity it can be shown that for $\gamma = 0$, n images get close to each star and one image moves to infinity and for $\gamma \neq 0$, $n + 1$ images get close to each star and $n + 1$ images move to infinity. That means that all image tracks of equation (A3) of Witt (1990) are connected with a star or are infinite long tracks which can be connected with one or more star. Additional loops can never appear because the number of images is conserved. But this means in particular that all real image tracks which belong to the observable images must be connected with a star or must be infinitely long. We already showed that there can only exist one real infinitely long image track. That means that all secondary image tracks must be connected with a star. Comparing Figure 13*b* with Figure 2*b* we see that the complex images convert into real images (and vice versa) at the critical curve. An exchange of images (real to complex or vice versa) is only allowed at the critical curve. In Figure 13*b* there are two cases where two image tracks cross each other at the critical curve. At the top cross, two complex solutions merge and convert into real solutions and separate again. At the cross below, the opposite situation happens.

REFERENCES

Blandford, R. D., & Narayan, N. 1986, ApJ, 310, 568
Chang, K. 1984, A&A, 130, 157
Chang, K., & Refsdal, S. 1979, Nature, 282, 561
———. 1984, A&A, 132, 168
Kayser, R., Refsdal, S., & Stabell, R. 1986, A&A, 166, 32
Kayser, R., & Witt, H. J. 1989, A&A, 221, 1
Lewis, G. F., Miralda-Escude, J., Richardson, D. C., & Wambsganss, J. 1992, MNRAS, submitted
Mao, S. 1992, ApJ, 389, 63
Paczyński, B. 1986, ApJ, 301, 503
Peacock, J. M. 1986, MNRAS, 223, 113
Petters, A. O. 1992, J. Math. Phys., 33, 1915
Rauch, K. P., Mao, S., Wambsganss, J., & Paczyński, B. 1992, ApJ, 386, 30
Schneider, P. 1987, ApJ, 319, 9
Schneider, P., & Weiss, A. 1986, A&A, 164, 237
———. 1987, A&A, 171, 49
———. 1992, A&A, 260, 1
Walsh, D., Carswell, R. F., & Weymann, R. J. 1979, Nature, 279, 381
Wambsganss, J. 1990, Ph.D. thesis, München, Max-Planck-Institut für Astrophysik
———. 1992, ApJ, 386, 19
Wambsganss, J., Witt, H. J., & Schneider, P. 1992, A&A, 258, 591
Witt, H. J. 1990, A&A, 236, 311
———. 1991, Ph.D. thesis, Hamburger Sternwarte, University of Hamburg
Witt, H. J., Kayser, R., & Refsdal, S. 1992, A&A, submitted
Young, P. 1981, ApJ, 244, 756